J. Marine Sci. Appl. (2014) 13: 388-393
DOI: 10.1007/s11804-014-1269-3

Numerical Investigation on Two-dimensional Boundary Layer Flow with Transition

Yong Zhao[1], Tianlin Wang[1] and Zhi Zong[2,3*]

1. Transportation Equipment and Ocean Engineering College, Dalian Maritime University, Dalian 116026, China
2. State Key Laboratory of Structural Analysis for Industrial Equipment, Dalian University of Technology, Dalian 116024, China
3. School of Naval Architecture, Dalian University of Technology, Dalian 116024, China

Abstract: As a basic problem in many engineering applications, transition from laminar to turbulence still remains a difficult problem in computational fluid dynamics (CFD). A numerical study of one transitional flow in two-dimensional is conducted by Reynolds averaged numerical simulation (RANS) in this paper. Turbulence model plays a significant role in the complex flows' simulation, and four advanced turbulence models are evaluated. Numerical solution of frictional resistance coefficient is compared with the measured one in the transitional zone, which indicates that Wilcox (2006) *k-ω* model with correction is the best candidate. Comparisons of numerical and analytical solutions for dimensionless velocity show that averaged streamwise dimensionless velocity profiles correct the shape rapidly in transitional region. Furthermore, turbulence quantities such as turbulence kinetic energy, eddy viscosity, and Reynolds stress are also studied, which are helpful to learn the transition's behavior.
Keywords: transitional boundary layer flow; Reynolds averaged numerical simulation (RANS); turbulence models; low Reynolds correction; Reynolds stress; eddy viscosity

Article ID: 1671-9433(2014)04-0388-06

1 Introduction

As a fundamental problem, transition prediction and its flow features are important in many engineering applications, such as ship hydrodynamics, aircraft, space vehicles, ground vehicles, turbo machinery blades, and wind turbines (Levin and Henningson, 2003; Ma *et al*., 2007; Ye *et al*., 2012). The frictional resistance on the wall in a turbulent boundary layer is much greater than that in the laminar flow. Therefore, a suppression or delay of the transition from laminar flow to turbulence can reduce the drag acting on the surface of structures, leading to an improvement of energy efficiency (Lee, 2002; Hackenberg *et al*., 1995). Hence, it is important to predict transition position and understand the corresponding physics. So, transitional flow has received much attention (Wang and Fu, 2009a, 2009b, 2011; Cao, 2009; Wassermann and Kloker, 2005). Besides experimental research (Klewicki *et al*., 2011), some numerical simulations based on Reynolds averaged numerical simulation (RANS) are conducted on the transition in the last decade (Biau *et al*., 2007; Jacobs and Durbin, 2000; Xiao *et al.,* 2006; Yang, 2012). However, due to the short length of transition zone with rapid variation of flow parameters, it raises higher request for the turbulent model in RANS method (Wang and Guo, 2012; Chen and Chen, 2010; Fan *et al*., 2011).

Therefore, in this paper an attempt is taken for the numerical investigation on transition by RANS with advanced turbulence models which have good performance in complicated flows' simulation, such as *k-ω* model, stress-*ω* model and their corresponding low Reynolds number correction versions (Wilcox, 2006). Despite that the geometric boundary has serious impact on the flow field, the fundamental understanding of the transition lies in the flat plate boundary flow. So the flat plate boundary layer flow is chosen as the research object. Hence one main purpose of this paper is to clarify the above four models' performance on predicting the frictional resistance along the plate by the available experimental data, and the second purpose is to understand the flow through the numerical study with the best model.

2 Governing equations and turbulence models

The two-dimensional incompressible and steady flow is taken into account. The corresponding governing equations are as follows:

$$\frac{\partial U}{\partial x}+\frac{\partial V}{\partial y}=0 \tag{1}$$

$$U\frac{\partial U}{\partial x}+V\frac{\partial U}{\partial y}=-\frac{1}{\rho}\frac{\partial p}{\partial x}+\left(\nu+\nu_T\right)\nabla^2 U \tag{2}$$

$$U\frac{\partial V}{\partial x}+V\frac{\partial V}{\partial y}=-\frac{1}{\rho}\frac{\partial p}{\partial y}+\left(\nu+\nu_T\right)\nabla^2 V \tag{3}$$

where U, V are streamwise and normal averaged velocity components; ρ, P are fluid density and pressure; ν, ν_T are molecular and turbulent eddy kinetic viscosities.

The *k-ω* model was firstly created independently by Kolmogorov and later by Saffman (1970), Wilcox has

Received date: 2014-05-23.
Accepted date: 2014-07-14.
Foundation item: Supported by the National Natural Science Foundation of China (Nos. 51309040, 51379025), and the Fundamental Research Funds for the Central Universities (Nos. 3132014224, 3132014318).
***Corresponding author Email:** zongzhi@dlut.edu.cn

continually refined and improved the model during the past three decades and demonstrated its accuracy for a wide range of turbulent flow (Wilcox and Alber, 1972; Wilcox, 1988; Wilcox, 2006). The latest version was put forward in 2006, termed as Wilcox (2006) *k-ω* model, the turbulent eddy viscosity:

$$\nu_T = k / \tilde{\omega}$$
$$\tilde{\omega} = \max(\omega, C_{\lim}\sqrt{\frac{2S_{ij}S_{ij}}{\beta^*}}) \quad (4)$$
$$C_{\lim} = \frac{7}{8}$$

Reynolds stress for incompressible flow is:

$$\tau_{ij} = 2\rho\nu_T S_{ij} \quad (5)$$

Turbulence kinetic energy equation:

$$U_j\frac{\partial k}{\partial x_j} = \tau_{ij}\frac{\partial U_i}{\partial x_j} - \beta^* k\omega + \frac{\partial}{\partial x_j}\left[\left(\nu + \sigma^*\frac{k}{w}\right)\frac{\partial k}{\partial x_j}\right] \quad (6)$$

Specific dissipation rate:

$$U_j\frac{\partial \omega}{\partial x_j} = \alpha\frac{\omega}{k}\tau_{ij}\frac{\partial U_i}{\partial x_j} - \beta\omega^2 + \frac{\sigma_d}{\omega}\frac{\partial k}{\partial x_j}\frac{\partial \omega}{\partial x_j} + \frac{\partial}{\partial x_j}\left[\left(\nu + \sigma\frac{k}{\omega}\right)\frac{\partial \omega}{\partial x_j}\right] \quad (7)$$

Closure coefficients and auxiliary relations:

$$\alpha = \frac{13}{25},\ \beta = \beta_0 f_\beta,\ \beta^* = \frac{9}{100},\ \sigma = \frac{1}{2},\ \sigma^* = \frac{3}{5},\ \sigma_d = \frac{1}{8} \quad (8)$$

$$\sigma_d = \begin{cases} 0, & \frac{\partial k}{\partial x_j}\frac{\partial \omega}{\partial x_j} \le 0 \\ \sigma_d, & \frac{\partial k}{\partial x_j}\frac{\partial \omega}{\partial x_j} > 0 \end{cases} \quad (9)$$

$$\beta_0 = 0.0708,\ f_\beta = \frac{1+85\chi_\omega}{1+100\chi_\omega},\ \chi_\omega \equiv \left|\frac{\Omega_{ij}\Omega_{jk}S_{ki}}{(\beta^*\omega)^3}\right| \quad (10)$$

where,

$$\Omega_{ij} = \frac{1}{2}\left(\frac{\partial U_i}{\partial x_j} - \frac{\partial U_j}{\partial x_i}\right),\quad S_{ij} = \frac{1}{2}\left(\frac{\partial U_i}{\partial x_j} + \frac{\partial U_j}{\partial x_i}\right) \quad (11)$$

As it can be easily verified, the quantity χ_ω is zero for two-dimensional flows. As to the solid wall, the boundary is under no-slip condition, i.e.

$$U = 0,\quad V = 0 \quad (12)$$

For the model equation, the boundary condition is specified as:

$$k = 0,\quad \omega = \frac{6\nu_w}{\beta_0 d^2} \quad (13)$$

where *d* is the distance from the nearest grid to the wall.

If the low Reynolds effect is included in the Wilcox (2006) *k-ω* model, the corrected closure coefficients are the following ones:

$$\alpha = \frac{5}{9}\cdot\frac{\alpha_0 + Re_T/R_\omega}{1+Re_T/R_\omega}\cdot\frac{1}{\alpha_0^*} \quad (14)$$

$$\beta^* = \frac{9}{100}\cdot\frac{5/18 + (Re_T/R_\beta)^4}{1+(Re_T/R_\beta)^4} \quad (15)$$

$$\beta = 3/40,\ \sigma^* = 1/2,\ \sigma = 1/2,\ \alpha_0^* = \beta/3 \quad (16)$$

$$\alpha_0 = 1/9,\ R_\beta = 8,\ R_k = 6,\ R_\omega = 2.61 \quad (17)$$

The quantity Re_T is turbulence Reynolds number defined by

$$Re_T = \frac{k}{\omega\nu} \quad (18)$$

In the meanwhile, Wilcox also improved the stress-*ω* model in 2006, which is an advanced model to solve the six Reynolds stress equations, including its low Reynolds number correction. For the detailed information of stress-*ω* model and its low Reynolds number correction, the interested readers may refer to Wilcox (2006).

3 Numerical experiment

3.1 Flow parameters

The flow parameters are the followings: the free stream air's velocity is 24.36 m/s, temperature is 293 K, density is 1.21 kg/m^3, pressure is 1.01×10^5 Pa, the length of the plate is 2.8 m, and the Reynolds number based on the flat's length 4.5×10^7. These parameters are consistent with the experiment by Schubauer and Klebanoff (1955) in order to validate our numerical experiment by their measured resistance coefficient. The coefficient is defined as $C_f = 2\tau_w/\rho U_\infty^2$, where $\tau_w = \rho\nu_t\partial U/\partial y|_{y=0}$. This physical quantity is determined by the derivative of velocity and eddy viscosity, thus it is a good candidate for checking numerical simulation.

3.2 Numerical method and the grids convergence validation

On the basis of laminar flow, the codes are supplemented to the four advanced models for calculating the transitional flow. Iterative algorithm is used to solve the equations according to the order of the momentum equations, the continuous equation and the turbulence model equations. A threshold value setting as 1×10^4 for streamwise averaged velocity's relative error between the two consecutive iterative values is used for checking numerical convergence. In the discrete equations, the second-order upwind difference format is used for the convection items and others are second-order central difference scheme. Uniform incoming velocity, free outflow, no-slip wall and periodic boundary conditions are defined for the boundary conditions. In order to check grids' convergence, three nested grids are used, with nodes number of 301×101, 151×51, and 75×25 to discrete the computational zone 2.8 m×0.03 m. It is found that the grids' convergence is satisfied for all the four turbulence models. For example, in the case of Wilcox (2006) *k-ω* model and its low Reynolds number correction, the frictional resistance coefficient along the plate is shown

in Fig. 1, indicating the numerical results' independence on the grids' density. So in the following calculation, the middle density grid is chosen, i.e. 151×51.

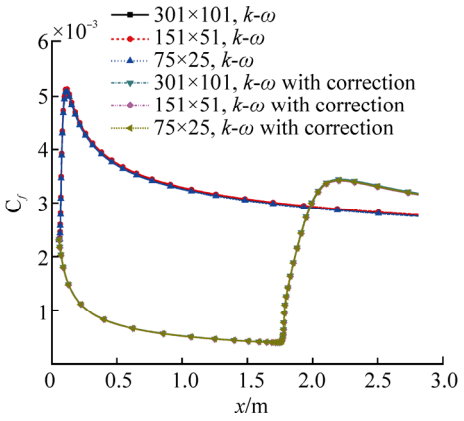

Fig. 1 The comparison of local frictional coefficient along the plate on three distributed grids

3.3 Models testing

In this section, the four candidate models are tested through the frictional resistance coefficients along the wall with the experimental ones in the transient zone particularly. Fig. 2 shows the comparisons in the case of Wilcox (2006) k-ω model and its low Reynolds number correction. As shown in Fig. 2, the result predicted by the low Reynolds number correction model is very close to the experimental ones. While in no correction version, the results are far from the experimental ones. Turbulence model is brought forward by the hypothesis of fully developed turbulence, and therefore it is natural to see that in the range of laminar flow, simulation without low Reynolds number is not able to give good prediction, and it will over-predict the frictional resistance.

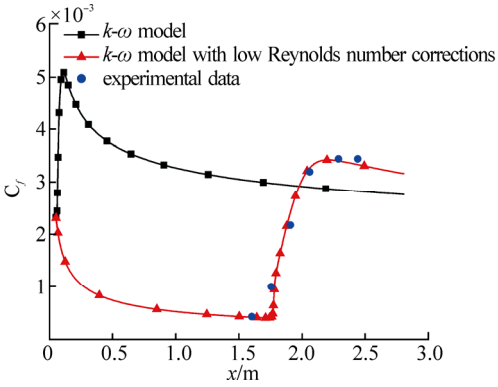

Fig. 2 The comparison of local frictional coefficient along the plate between Wilcox (2006) k-ω model and its low Reynolds number correction's numerical and experimental results

The similar comparison is conducted in the case of stress-ω model and its low Reynolds number correction version is shown in Fig. 3. In addition, over prediction appears again in the case of no low Reynolds correction. But in the corrected version, the numerical simulation underestimates the coefficients. Compared to Fig. 2, it is concluded that the Wilcox (2006) k-ω model with low Reynolds number correction is the best candidate model to calculate the transitional flow from laminar to turbulence. Therefore, the following numerical results are calculated by this model in this paper.

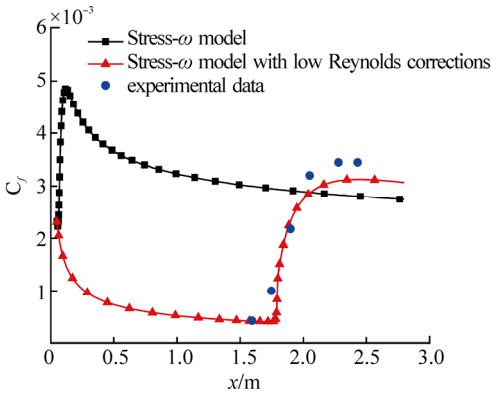

Fig. 3 The comparison of local frictional coefficient along the plate between stress-ω model and its low Reynolds number correction's numerical and experimental results

3.4 Results and discussion

For the purpose of understanding the transient flow, in this section, the velocity profiles or its dimensionless ones at several positions, eddy viscous coefficient and turbulent kinetic energy's distribution in the boundary layer will be studied. Fig. 4 shows the averaged streamwise velocity profiles at the position of x=1.7, 1.9, 2.1 m in transitional zone. As the distance increases, profile becomes more and more plump, which is in line with the qualitative analysis. Meanwhile, it can be noticed that the variation among these profiles is changed quickly in the transition and it is thought that this brings the main difficulty for turbulence models' numerical prediction.

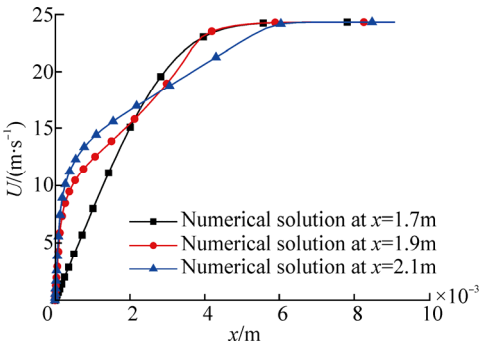

Fig. 4 Comparisons of averaged stream-wise velocity profiles near the transition

It is known the averaged dimensionless velocity has

analytical solution. Defining the dimensionless velocity U^+ and the distance from the plate y^+ as:

$$U^+ = U/u_\tau, \quad y^+ = u_\tau y/\nu \tag{19}$$

where $u_\tau = \sqrt{\tau_w/\rho}$, then this dimensionless velocity U^+ satisfies the following formula in the viscous sub-layer and turbulent log-layer, respectively for a fully developed turbulent boundary layer flow (Schlichting, 2003).

$$U^+ = y^+, \quad U^+ = \frac{1}{\kappa}\ln y^+ + C \tag{20}$$

Correlation of measurements indicates $C \approx 5.0$ for smooth surface and $\kappa \approx 4.1$ for smooth and rough surfaces. These analytical solutions will be used in fully turbulent flow as reference for the transitional flow's behavior.

The profiles on some typical positions are investigated, i.e. in the zone of laminar (shown in Fig. 5), transitional (in Fig. 6) and turbulent flow (in Fig. 7). In Fig. 5, both profiles at position x=1.0, 1.5 m are overlapped quite well in the region where y^+<30; meanwhile, they nearly coincide with the viscous sub-layer $U^+=y^+$, according to the property of laminar flow.

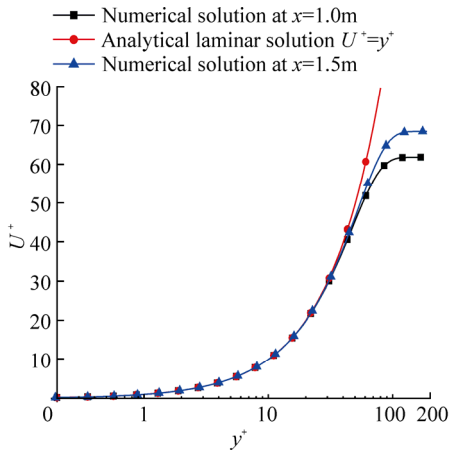

Fig. 5 Comparison of dimensionless averaged stream-wise velocity numerical profiles in laminar zone and analytical solution for laminar flow

In Fig. 6, the profiles in the transitional zone are plotted. The three profiles differ much from each other. The profile at x=1.7 m is quite similar to laminar flow's behavior. While in profiles at positions of x=1.8 m and 1.9 m, the departure increases after y^+=40, and both of them do not meet the turbulent logarithmic solution. Meanwhile, the viscous sub-layer is decreased by y^+<7, indicating that transitional flow is in a chaotic and disordered state.

In Fig. 7, profiles on position x=2.0, 2.5 m in turbulence region are plotted. It is found that the numerical result agrees with the turbulent logarithmic solution well, as well as the viscous sub-layer solution where y^+<7. As indicated by Figs. 5–7, the numerical results agree with qualitative and quantitative analysis.

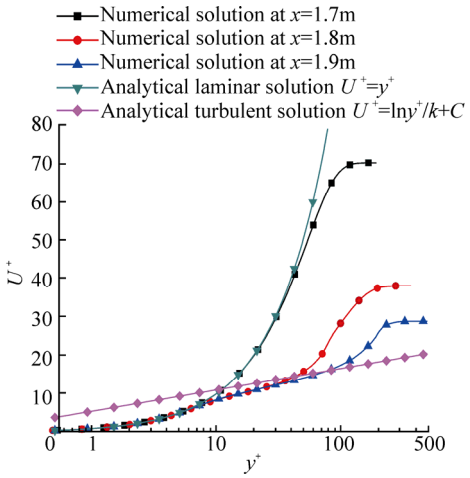

Fig. 6 Comparison of dimensionless averaged stream-wise velocity numerical profiles in transitional zone and analytical solutions both for laminar and turbulent flow

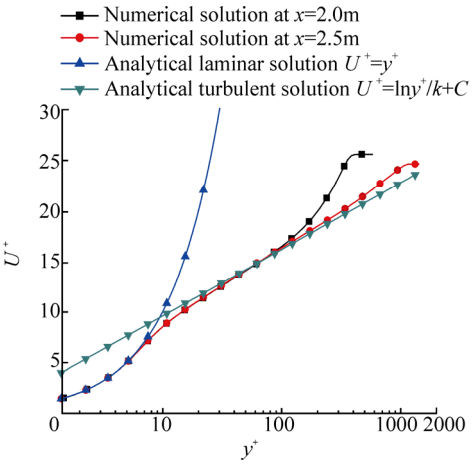

Fig. 7 Comparison of dimensionless averaged stream-wise velocity's numerical profiles in turbulence zone and analytical solutions both for laminar and turbulent flow

Fig. 8 shows contour lines of the ratio between eddy viscous and molecular viscous coefficient. Turbulent viscous coefficient is the key quantity in RANS. Larger value indicates turbulence is more fully developed. It can be noticed that this value undergoes a great increase at the position x=1.7 m, which is consistent with the position where local frictional resistance coefficient increases obviously in Fig. 2. Furthermore, based on the eddy viscous coefficient's distribution, the boundary layer flow's structure can be observed. After the transition, the flow becomes active and the fully developed turbulence is located in the middle of the latter part.

The turbulent kinetic energy is also associated with turbulence development level. Fig. 9 shows the contour lines of turbulent kinetic energy. Similar to turbulent eddy viscous coefficient distribution, the kinetic energy experiences a sharp raise at the position where transition occurs. It can be

noticed that the larger value part is located near the wall surface, which is different from turbulence eddy viscosity coefficient's distribution, where the larger value is distributed in the middle of the latter part.

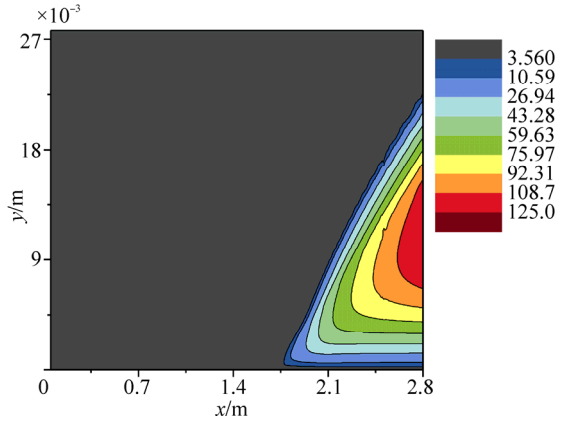

Fig. 8 Contour lines of the ratio between eddy and molecular viscous coefficient

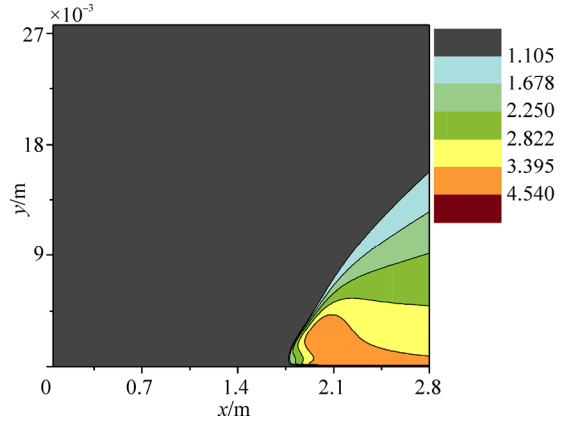

Fig. 9 Contour lines of turbulent kinetic energy

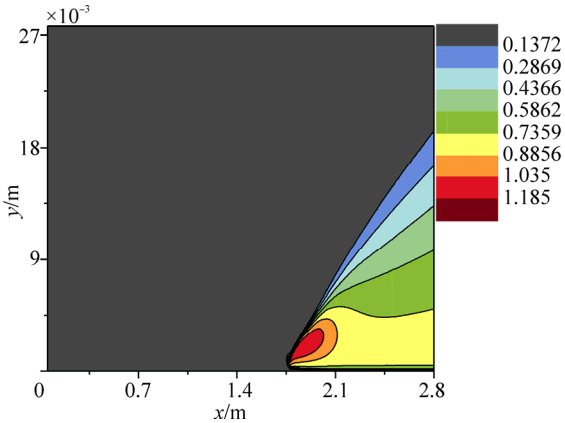

Fig. 10 Contour lines of the ratio between tangential Reynolds stress and frictional resistance stress τ_w

Contour lines of the ratio between tangential Reynolds stress and skin resistance stress τ_w are shown in Fig. 10. Tangential Reynolds stress' distribution is similar to that of turbulent kinetic energy and it's more concentrated in the transitional zone.

4 Conclusions

Numerical computations are performed to investigate transitional flow from laminar flow to turbulence in two-dimensional boundary layer flow by RANS. The simulation applies the Wilcox (2006) k-ω and stress-ω turbulence models and corresponding low Reynolds number correction. By comparison of numerical and experimental local frictional resistance coefficients, it is found that Wilcox (2006) k-ω model with correction is the best model to simulate this complicated flow. By comparing the dimensionless $U^+ \sim y^+$ profiles at particular positions, the flow in transitional zone corrects the velocity profile rapidly and the flow is more chaotic and disordered; in the two ends, i.e. laminar and turbulence zone, the $U^+ \sim y^+$ profiles are in line with the corresponding analytical solution. The characteristics of turbulence, such as turbulent kinetic energy, eddy viscosity and Reynolds stress are also studied, which indicate that most of the larger values of these quantities are concentrated in the transitional and turbulence regions. However, many factors, such as pressure gradient, turbulent intensity and wall surface roughness can affect transition remarkably, which will be included in the future research.

References

Biau D, Arnal D, Vermeersch O (2007). A transition prediction model for boundary layers subjected to free-stream turbulence. *Aerospace Science and Technology*, **11**(5), 370-375.

Cao W (2009). A study of the transition prediction of hypersonic boundary layer on plane and wedge flow. *Acta Aerodynamica Sinica*, **27**(5), 516-523. (in Chinese)

Chen JC, Chen WJ (2010). The complex nature of turbulence transition in boundary layer flow over a flat surface. *International Journal of Emerging Multidisciplinary Fluid Sciences*, **2**(2),183-203.

Fan M, Cao W, Fang XJ (2011). Prediction of hypersonic boundary layer transition with variable specific heat on plane flow. *Science China: Physics, Mechanics and Astronomy,* **54**(11), 2064-2070.

Hackenberg PJ, Rioual L, Tutty OR (1995). The automatic control of boundary layer transition experiments and computation. *Applied Scientific Research*, **54**(4), 293-311.

Jacobs RG, Durbin PA (2000). Simulations of bypass transition. *Journal of Fluid Mechanics*, **428**, 185-212.

Klewicki J, Ebner R, Wu X (2011). Mean dynamics of transitional boundary-layer flow. *Journal of Fluid Mechanics*, **682**, 617-651.

Lee KH (2002). Control of boundary layer flow transition via distributed reduced-order controller. *KSME International Journal*, **16**(12), 1561-1575.

Levin O, Henningson DS (2003). Exponential vs algebraic growth and transition prediction in boundary layer flow. *Flow, Turbulence and Combustion*, **70**, 183-210.

Ma HD, Pan HL, Wang Q (2007). Study of flow transition process induced by oblique wave instability in a supersonic flat-plate

boundary layer. *Chinese Journal of Theoretical and Applied Mechanics*, **39**(2), 153-157. (in Chinese)

Saffman PG (1970). A model for inhomogeneous turbulent flow. *Proceedings of the Royal Society of London, Series A: Mathematical and Physical Sciences*, **317**, 417-433.

Schlichting H (2003). *Boundary-layer theory*. 8th edtion. Springer, New York, USA, 272-273.

Schubauer GB, Klebanoff PS (1955). *Contributions on the mechanics of boundary-layer transition*. NACA technical reports, No. 1289.

Wang L, Fu S (2009a). Modelling flow transition in a hypersonic boundary layer with Reynolds-averaged Navier-Stokes approach. *Science in China, Series G: Physics, Mechanics and Astronomy*, **52**(5), 768-774.

Wang L, Fu S (2009b). New transition/turbulence model for the flow transition in supersonic boundary layer. *Chinese Journal of Theoretical and Applied Mechanics*, **41**(2), 162-168. (in Chinese)

Wang L, Fu S (2011). Development of an intermittency equation for the modeling of the supersonic/hypersonic boundary layer flow transition. *Flow, Turbulence and Combustion*, **87**(1), 165-187.

Wang WX, Guo RW (2012). Study of flow characteristics of hypersonic inlet based on boundary layer transition. *Acta Aeronautica et Astronautica Sinica*, **33**(10), 1772-1780. (in Chinese)

Wassermann P, Kloker M (2005). Transition mechanisms in a three-dimensional boundary-layer flow with pressure-gradient changeover. *Journal of Fluid Mechanics*, **530**, 265-293.

Wilcox DC (1988). Reassessment of the scale determining equation for advanced turbulence models. *American Institute of Aeronautics and Astronautics Journal*, **26**(11), 1299-1310.

Wilcox DC (2006). *Turbulence modeling for CFD*. 3rd edition. DCW Industries, La Canada, CA, USA, 124-126.

Wilcox DC, Alber IE (1972). A turbulence model for high speed flows. *Proceedings of the Heat Transfer and Fluid Mechanics Institute*, Northridge, California, USA, 231-252.

Xiao ZX, Chen HX, Li QB, Fu S (2006). A primary study of transitions in turbulence models. *Chinese Journal of Computational Physics*, **23**(1), 61-65. (in Chinese)

Yang ZY (2012). Numerical study of transition process in a separated boundary layer on a flat plate with two different leading edges. *WSEAS Transactions on Applied and Theoretical Mechanics*, **7**(1), 49-58.

Ye HX, Shen ZR, Wan DC (2012). Numerical prediction of added resistance and vertical ship motions in regular head waves. *Journal of Marine Science and Application*, **11**(4), 410-416.

Author biographies

Yong Zhao is a lecturer at Transportation Equipment and Ocean Engineering College, Dalian Maritime University. His research interests include ship hydrodynamics, turbulence models and numerical simulation based on wavelet method.

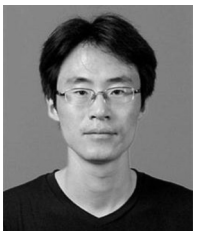

Tianlin Wang is a prefessor at Transportation Equipment and Ocean Engineering College, Dalian Maritime University. His research interests include hydrodynamics on underwater glider and computational fluid dynamics.

Zhi Zong is presently a professor and dean at School of Naval Architecture, Dalian University of Technology. He has been the principal investigator of a large variety of funded research work regarding the design and optimization of conventional and unconventional vessels. His research interests include hydrodynamics, underwater explosion and numerical methods in CFD, *etc*. His activities are documented by an extensive publication record of scientific papers, books, technical reports, and papers at international conferences (over 200 publications and two English monographs). He is the editorial advisory board member of several academic journals, including Journal of Hydrodynamics, Journal of Marine Science and Application and so on.